

Top quark mass definition and $t\bar{t}$ production near threshold at the NLC

Oleg Yakovlev^{1,a} and Stefan Groote^{2,3,b}

¹ Randall Laboratory of Physics, University of Michigan,
Ann Arbor, Michigan 48109-1120, USA

² Institut für Physik der Johannes-Gutenberg-Universität,
Staudinger Weg 7, 55099 Mainz, Germany

³ Floyd R. Newman Laboratory, Cornell University,
Ithaca, NY 14853, USA

Abstract

We suggest an infrared-insensitive quark mass, defined by subtracting the soft part of the quark self energy from the pole mass. We demonstrate the deep relation of this definition with the static quark-antiquark potential. At leading order in $1/m$ this mass coincides with the PS mass which is defined in a completely different manner. Going beyond static limit, the small normalization point introduces recoil corrections which are calculated here as well. Using this mass concept and other concepts for the quark mass we calculate the cross section of $e^+e^- \rightarrow t\bar{t}$ near threshold at NNLO accuracy adopting three alternative approaches, namely (1) fixing the pole mass, (2) fixing the PS mass, and (3) fixing the new mass which we call the $\overline{\text{PS}}$ mass. We demonstrate that perturbative predictions for the cross section become much more stable if we use the PS or the $\overline{\text{PS}}$ mass for the calculations. A careful analysis suggests that the top quark mass can be extracted from a threshold scan at NLC with an accuracy of about 100 – 200 MeV.

^ae-mail: yakovlev@umich.edu

^be-mail: groote@thep.physik.uni-mainz.de

1 Introduction

One of the main goals of future e^+e^- and $\mu^+\mu^-$ colliders such as the Next Linear Collider (NLC) and the Future Muon Collider (FMC) will be to measure and to determine the properties of the top quark which was first discovered at the Tevatron [1] with a mass of $m = 174.3 \pm 5$ GeV [2]. Although the top quark will be studied at the LHC and the Tevatron (RUN-II) with an expected accuracy for the mass of 2–3 GeV, the *most accurate measurement* of the mass with an accuracy of 0.1% (100 – 200 MeV) is expected to be obtained only at the NLC [3].

Due to the large top quark width, the top-antitop pair cannot hadronize into toponium resonances. The cross section appears therefore to have a smooth line-shape showing only a moderate $1S$ peak. In addition the top quark width serves as an infrared cutoff [4, 5] and as a natural smearing over the energy [6]. As a result, the nonperturbative QCD effects induced by the gluon condensate are small [7, 8], allowing us to calculate the cross section with high accuracy by using perturbative QCD even in the threshold region. Many theoretical studies at LO and NLO have been done in the past for the total cross section [4, 5, 7, 9], for the momentum distribution [10, 11], also accounting for electro-weak corrections [12, 13, 14], and for the complete NLO correction including non-factorizable corrections [15, 16, 17, 18].

Recently, the NNLO analysis of the inclusive threshold production cross section has been reported [19, 20, 21, 22, 23, 24, 25]. The results of the NNLO analysis are summarized in a review article [26]. To summarize the results for a standard approach using the pole mass, the NNLO corrections are uncomfortably large, spoiling the possibility for the top quark mass extraction at NLC with good accuracy because the $1S$ peak is shifted by about 0.5 GeV by the NNLO, the last known correction. One of the main reasons for this is the usage of the pole mass in the calculations. It was realized that such type of instability is caused by the fact that the pole mass is a badly defined object within full QCD [27, 28].

In this paper we suggest a definition of the quark mass alternative to the pole mass. We call it $\overline{\text{PS}}$ mass because in the static limit this mass coincides with the potential subtracted (PS) mass, even though the PS mass is defined in a different manner [29]. This is the reason why we include both of them in this paper. The ratio of the small normalization point and the mass introduce relativistic corrections (called recoil corrections) which result in the difference between the two masses at higher orders in $1/m$. In contrast to the pole mass, the PS and the $\overline{\text{PS}}$ mass are not sensitive to non-perturbative QCD effects. We derive recoil corrections to the relation of the pole mass to the $\overline{\text{PS}}$ mass and demonstrate that perturbative predictions for the cross section become much more stable at higher orders of QCD (shifts are below 0.1 GeV) if we use the PS or $\overline{\text{PS}}$ mass for the calculations, as it is the case for any of the other threshold masses. This understanding removes one of the obstacles for the accurate top quark mass measurement and it can be expected that the top quark mass will be extracted from a threshold scan at NLC with an accuracy of about 100 – 200 MeV. The necessity of isolating the IR contributions in the mass calculation and the consideration of a short distance mass have been studied intensively [28, 29, 30, 31, 32]. The applications of the PS, LS and $1S$ mass have been reported recently by several groups [22, 23, 24, 33, 34] and reviewed in Ref. [26]. The detailed comparison of our results using the PS mass with results of other groups have been performed in Ref. [26] so that we refer the reader to this reference for details.

This paper is therefore devoted to two subjects. First, we define the $\overline{\text{PS}}$ mass which allows us to calculate recoil corrections near the threshold. Second, we calculate the cross section for $e^+e^- \rightarrow t\bar{t}$ near threshold with NNLO accuracy using three alternative mass concepts, i.e. (1) the pole mass, (2) the static PS mass, and (3) the new $\overline{\text{PS}}$ mass. The results of the first

approach has already been reported in Ref. [21], the *preliminary* results for the top quark pair production near threshold using the static PS mass were presented at the workshop “Physics at Linear Colliders” [33, 26] by one of the authors. The results on the second and third alternative concepts which we present here are new.

The paper is organized as follows: In Sec. 2 we give the definition of the $\overline{\text{PS}}$ mass in terms of the soft part of the self energy and calculate the leading order contribution. In Sec. 3 we calculate the two-loop corrections and present our final result. In Sec. 4 we use the obtained results for the analysis of the top quark pair production. In Sec. 5 we give our conclusions. The Appendix contains explicit expressions for the coefficients which occur in the text.

2 Mass definitions

The top quark mass is an input parameter of the Standard Model. Although it is widely accepted that the quark masses are generated due to the Higgs mechanism, the value of the mass cannot be calculated from the Standard Model. Instead, quark masses have to be determined from the comparison of theoretical predictions and experimental data.

It is important to stress that there is no unique definition of the quark mass. Because the quark cannot be observed as a free particle like the electron, the quark mass is a purely theoretical notion and depends on the concept adopted for its definition. The best known definitions are the pole mass and the $\overline{\text{MS}}$ mass. However, both definitions are not adequate for the analysis of top quark production near threshold. The pole mass should not be used because it has the renormalon ambiguity and cannot be determined more accurately than 300 – 400 MeV [27, 28] (see also Refs. [29, 35]). The $\overline{\text{MS}}$ mass is an Euclidean mass, defined at high virtuality, and therefore destroys the non-relativistic expansion. Instead, it was recently suggested to use threshold masses like the low scale (LS) mass [28], the potential subtracted (PS) mass [29], or one half of the perturbative mass of a fictitious 1^3S_1 ground state (called $1S$ mass) [23]. In this paper we study the static PS mass suggested in Ref. [29],

$$m_{\text{PS}} = m_{\text{pole}} - \delta m_{\text{PS}} \quad \text{with} \quad \delta m_{\text{PS}} = -\frac{1}{2} \int^{|\vec{k}| < \mu_f} \frac{d^3 k}{(2\pi)^3} V_C(|\vec{k}|) \quad (1)$$

where V_C is the quark-antiquark Coulomb potential. In order to understand why this mass definition is more adequate than the pole mass and to see that the pole mass is very sensitive to long distance effects, it is enough to consider the one-loop expression for the self energy diagram. Taking the residue in k_0 , one obtains a soft self energy contribution which comes from momenta k with $|\vec{k}| < \Lambda_{\text{QCD}}$,

$$\delta m = 4\pi\alpha_s C_F \int_{|\vec{k}| < \Lambda_{\text{QCD}}} \frac{d^3 k}{(2\pi)^3} \frac{1}{2|\vec{k}|^2} = \frac{\alpha_s C_F}{\pi} \Lambda_{\text{QCD}}. \quad (2)$$

We observe that the pole mass has a non-perturbative uncertainty of order Λ_{QCD} which then penetrates into consequent perturbative QCD calculations. It is easy to realize that the PS mass is free of this ambiguity. Indeed, the term δm in Eq. (2) cancels in the definition of the PS mass as given in Eq. (1) as well as in the combination $2m_{\text{pole}} + V(r)$. The definition in Eq. (1) has been given in Ref. [29] but has already been discussed implicitly in Ref. [28]. The remarkable step made in Ref. [29] is to use this definition beyond one-loop order. It has been

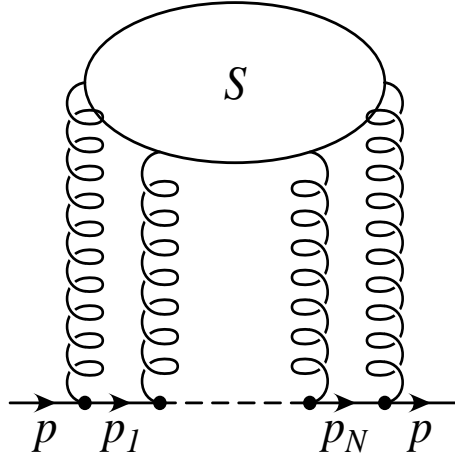


Figure 1: The general structure of the self energy diagram of a quark

proven in Ref. [29] that the cancellation of the infrared QCD contributions to the PS mass in Eq. (1) holds even at higher loop orders.

In this paper we suggest a natural definition of a short distance quark mass near threshold. Our objective is that the definition should be gauge independent and well-defined within quantum field theory so that radiative and relativistic corrections can be calculated in a systematic way. Nevertheless, we stress that both concepts, as well as the other concepts mentioned before, are equivalently applicable to considerations near the quark production threshold.

2.1 The $\overline{\text{PS}}$ mass

We define

$$m_{\overline{\text{PS}}} = m_{\text{pole}} - \delta m_{\overline{\text{PS}}} \quad \text{with} \quad \delta m_{\overline{\text{PS}}} = \Sigma_{\text{soft}}(\not{p}) \Big|_{\not{p}=m} \quad (3)$$

where Σ_{soft} is the soft part of the heavy quark self energy which is defined as the part where at least one of the heavy quark propagators is on-shell. A more precise definition is given below. We will show that the static PS mass and the new $\overline{\text{PS}}$ mass definition coincide at leading order in $1/m$. At the same time we stress that the new definition accounts for recoil corrections of orders $1/m$ and $1/m^2$. But first we describe the physical picture and discuss the structure of the quark self energy shown in Fig. 1.

The starting point of our considerations is an on-shell quark with mass m and momentum p (i.e. $p^2 = m^2$) which we consider to be at rest, $p = (m, \vec{0})$. This quark interacts with a number of gluons, the subdiagram S displayed in Fig. 1 describes the interaction between the gluons. In general the quark lines between the interaction points represent virtual quark states. However, if the virtual quark comes very close to the mass shell and the total momentum of the cloud of virtual gluons becomes soft, this situation gives rise to long-distance nonperturbative QCD interactions. The described (virtual) contributions result in the soft part of the self energy, Σ_{soft} . For a precise definition we start with a general self energy diagram as shown in Fig. 1,

$$-i\Sigma(\not{p}) = \int \prod_{m=1}^M \frac{d^4 l_m}{(2\pi)^4} S_{\{\alpha_n\}}^{\{a_n\}}(\{l_m\}) \left(-ig_s \gamma^{\alpha_{N+1}} T_{a_{N+1}}\right) \prod_{n=N}^1 \frac{i}{\not{p}_n - m} \left(-ig_s \gamma^{\alpha_n} T_{a_n}\right) \quad (4)$$

where the last factor is a non-commutative product with decreasing index n . The line momenta k_n are linear combinations of the gluon loop momenta l_m , the particular representation is specified by the structure S . The symbol $\{l_m\}$ means the set of all these loop momenta, the same symbol is used for the Lorentz and color indices. In general we have $M \leq N$ which means that line momenta can be correlated. The momenta of the virtual quark states are given by $p_n = p + k_n$. Taking this as the starting point we define

$$\begin{aligned}
-i\Sigma_{\text{soft}}(\not{p}) &= \sum_{i=1}^N \int \prod_{m=1}^M \frac{d^4 l_m}{(2\pi)^4} S_{\{\alpha_n\}}^{\{a_n\}}(\{l_m\}) \left(-ig_s \gamma^{\alpha_{N+1}} T_{a_{N+1}}\right) \prod_{n=N}^{i+1} \frac{i}{\not{p}_n - m} \left(-ig_s \gamma^{\alpha_n} T_{a_n}\right) \times \\
&\times i(\not{p}_i + m) \left(-i\pi\delta(p_i^2 - m^2)\right) \left(-ig_s \gamma^{\alpha_i} T_{a_i}\right) \prod_{n=i-1}^1 \frac{i}{\not{p}_n - m} \left(-ig_s \gamma^{\alpha_n} T_{a_n}\right). \quad (5)
\end{aligned}$$

This equation is the definition of the soft part of the quark self energy. One can derive this expression from Eq. (4) by using the identity

$$\frac{1}{p^2 - m^2 + i\epsilon} = -i\pi\delta(p^2 - m^2) + P\left(\frac{1}{p^2 - m^2}\right) \quad (6)$$

and the fact that the principal value integral does not give any infrared sensitive contribution. The delta function can be used to remove the integration over the zero component of k_i . In order to parameterize the softness of the gluon cloud we impose a cutoff on the spatial component, $|\vec{k}_i| < \mu_f$, and indicate this by a label μ_f written at the upper limit of the three-dimensional integral. This cutoff μ_f is also known as *factorization scale*. So we can rewrite Eq. (5) as

$$\Sigma_{\text{soft}}(\not{p}, \mu_f) = -\frac{1}{2} \sum_{i=1}^N \int^{\mu_f} \frac{d^3 k_i}{(2\pi)^3} V(\vec{k}_i, p) \quad (7)$$

where

$$\begin{aligned}
V(\vec{k}_i, p) &:= - \int \prod_{m=1}^{M-1} \frac{d^4 l_m}{(2\pi)^4} S_{\{\alpha_n\}}^{\{a_n\}}(\{l_m\}) \left(-ig_s \gamma^{\alpha_{N+1}} T_{a_{N+1}}\right) \prod_{n=N}^{i+1} \frac{i}{\not{p}_n - m} \left(-ig_s \gamma^{\alpha_n} T_{a_n}\right) \times \\
&\times \frac{\not{p}_i + m}{2p_i^0} \left(-ig_s \gamma^{\alpha_i} T_{a_i}\right) \prod_{n=i-1}^1 \frac{i}{\not{p}_n - m} \left(-ig_s \gamma^{\alpha_n} T_{a_n}\right). \quad (8)
\end{aligned}$$

The range of the index m is reduced by one which indicates that one of the loop momenta is extracted as line momentum of the i -th line. In the following we deal with the different realizations of this compact expression. As we will see explicitly, the function $V(\vec{k}, p)$ occurring as integrand can be seen as quark-antiquark potential where we have summed over the spin of the tensor product of a final state with an initial state. Because the static quark-antiquark potential is used in a similar way in Ref. [29], we recover the result of Ref. [29] in the static limit. However, there is no kind of hierarchical order between both concepts because both solve the afore mentioned problems with non-perturbative uncertainties of the order $O(\Lambda_{\text{QCD}})$. The role of non-perturbative effects of the order $1/m$ have to be studied elsewhere.

2.2 The leading order perturbative contribution

The leading order contribution to the self energy of the quark is given by

$$\Sigma(\not{p}) = i \int \frac{d^4 k}{(2\pi)^4} \left(-ig_s \gamma_\alpha T_a\right) \frac{i}{\not{p} + \not{k} - m} \left(-ig_s \gamma^\alpha T_a\right) \frac{-i}{k^2} \quad (9)$$

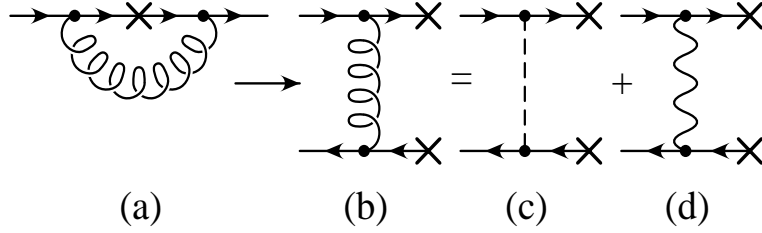


Figure 2: Leading order contribution to the quark self energy (a) and to the quark-antiquark potential (b). The cross indicates the point where we cut the quark line by imposing an on-shell condition to the virtual quark state. The gluon propagator can be decomposed in a Coulomb propagator (c) and a transverse propagator (d).

where Feynman gauge is used for the gluon. The soft contribution thus reads

$$\begin{aligned}\Sigma_{\text{soft}}(\not{p}) &= -ig_s^2 C_F \int \frac{d^4 k}{(2\pi)^4 k^2} \gamma_\alpha (\not{p} + \not{k} + m) \gamma^\alpha \left(-i\pi \delta \left((p+k)^2 - m^2 \right) \right) = \\ &= -\pi g_s^2 C_F \int \frac{d^4 k}{(2\pi)^4 k^2} (-2(\not{p} + \not{k}) + 4m) \delta \left((p+k)^2 - m^2 \right).\end{aligned}\quad (10)$$

The projector $(1 + \gamma^0)/2$ which represents the on-shell quark at rest can be placed at the left and at the right of the Dirac structure and will lead to a further simplification. In terms of the zero component of the momentum k the Dirac delta function has two zeros $k_0 = k_+$ and $k_0 = k_-$ with

$$k_\pm := \pm \sqrt{\kappa^2 + m^2} - m \quad (11)$$

where $\kappa = |\vec{k}|$. The delta function is therefore written as

$$\delta \left((p+k)^2 - m^2 \right) = \frac{1}{2\sqrt{\kappa^2 + m^2}} \left(\delta(k_0 - k_+) + \delta(k_0 - k_-) \right). \quad (12)$$

The procedure which is done here is shown in Fig. 2(a-b). The cross indicates that we cut the line at this point by imposing the on-shell condition to the corresponding (virtual) momentum. The diagram then proceeds to a quark-antiquark interaction diagram where we have kept the crosses to indicate the position of the cut line. This line carries the momentum $p+k$ while the other two external lines carry the momentum p . Accordingly we obtain

$$\Sigma_{\text{soft}}(\not{p}, \mu_f) = -\frac{1}{2} \int^{\mu_f} \frac{d^3 k}{(2\pi)^3} V(\vec{k}, p), \quad V(\vec{k}, p) = V_+(\vec{k}, p) + V_-(\vec{k}, p) \quad (13)$$

where

$$V_\pm(\vec{k}, p) = g_s^2 C_F \frac{-(m + k_\pm) + 2m}{\sqrt{m^2 + \kappa^2} (k_\pm^2 - k^2)} = \frac{g_s^2 C_F (\sqrt{m^2 + \kappa^2} \mp 2m)}{2m \sqrt{m^2 + \kappa^2} (\sqrt{m^2 + \kappa^2} \mp m)}. \quad (14)$$

For $m \ll \mu_f$ the restriction of the three-dimensional integral allows for an expansion in κ/m . We obtain

$$\begin{aligned}V_+(\vec{k}, p) &= -4\pi\alpha_s C_F \left\{ \frac{1}{\kappa^2} - \frac{3}{4m^2} + O\left(\frac{\kappa^2}{m^4}\right) \right\}, \\ V_-(\vec{k}, p) &= -4\pi\alpha_s C_F \left\{ -\frac{3}{4m^2} + O\left(\frac{\kappa^2}{m^4}\right) \right\}\end{aligned}\quad (15)$$

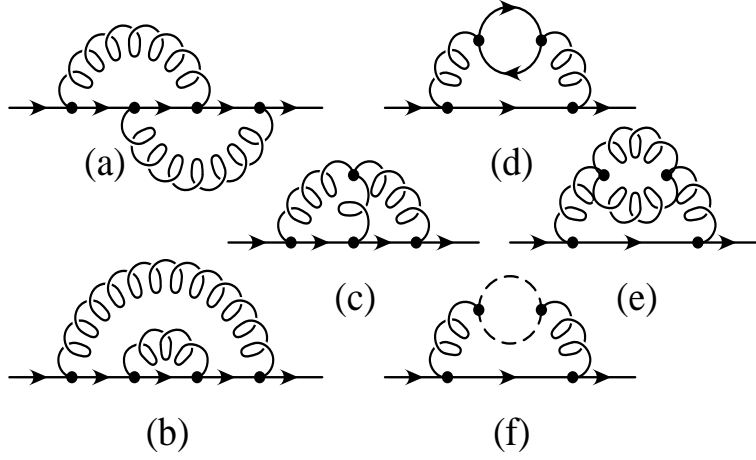


Figure 3: Two-loop contributions to the quark self energy

and therefore

$$V(\vec{k}, p) = -4\pi\alpha_s C_F \left\{ \frac{1}{\kappa^2} - \frac{3}{2m^2} + O\left(\frac{\kappa^2}{m^4}\right) \right\}. \quad (16)$$

The first term is the Coulomb potential for a quark-antiquark interaction. The second term can be related to the Breit-Fermi potential of the quark-antiquark interaction [36] by summing over the spin states of the tensor product of the final quark and the final antiquark state and using the same kinematic constraints. Moreover, one can identify $V_+(\vec{k}, p)$ with the scattering potential and $V_-(\vec{k}, p)$ with the annihilation potential.

One can integrate this radial symmetric potential over the space components and end up with an expansion in $1/m$. Note that there are no contributions to odd powers of $1/m$. But one can also integrate the exact expressions for $V_{\pm}(\vec{k}, p)$ in Eq. (14) up to the factorization scale μ_f and obtain

$$\Sigma_{\text{soft}}(\mu_f) = \frac{\alpha_s C_F}{2\pi} m \left\{ 3 \ln \left(\frac{\mu_f}{m} + \sqrt{\frac{\mu_f^2}{m^2} + 1} \right) - \frac{\mu_f}{m} \sqrt{\frac{\mu_f^2}{m^2} + 1} \right\}. \quad (17)$$

The expansion of this expression in small values of μ_f/m results in

$$\Sigma_{\text{soft}}(\mu_f) = \frac{\alpha_s C_F}{\pi} \mu_f \left\{ 1 - \frac{\mu_f^2}{2m^2} \right\}. \quad (18)$$

The first term reproduces the result given in Ref. [29] to leading order in α_s while the second term is the recoil correction to the static limit in this order of perturbation theory. This second term is related to the Breit-Fermi potential but does not coincide with it.

3 Two loop contributions

To take a step beyond the leading order perturbation theory, we consider two-loop diagrams for the heavy quark self energy as shown in Fig. 3. We calculate them in Coulomb gauge, even though we stress that our final result is gauge invariant. The gluon propagator in Coulomb gauge is given by

$$G_{00}^{ab}(k) = \frac{i\delta^{ab}}{k^2}, \quad G_{ij}^{ab}(k) = \frac{i\delta^{ab}}{k^2} \left(\delta_{ij} - \frac{k_i k_j}{k^2} \right), \quad i, j = 1, 2, 3. \quad (19)$$

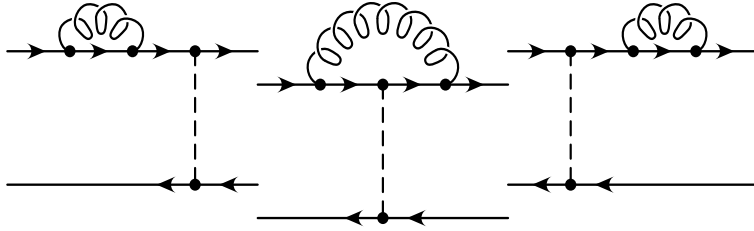


Figure 4: Diagrams which cancel due to the classical Ward identity

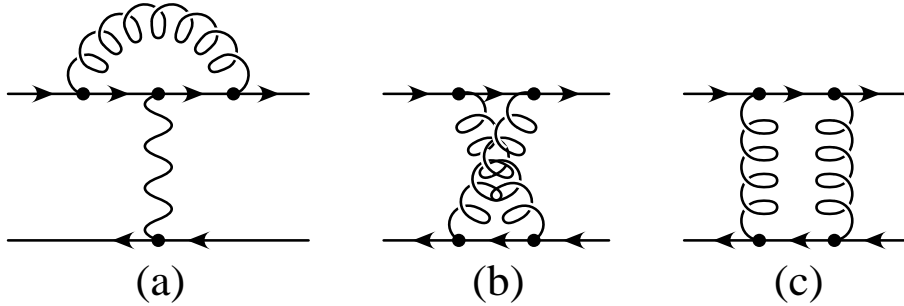


Figure 5: Diagrams which contribute to order $O(\mu_f^2/m^2)$

The use of Coulomb gauge splits up the gluon propagators into a Coulomb term (Coulomb gluon) and a transverse term (transverse gluon) where the first one couples to the quark via the time components only. This splitting is shown in Fig. 2(b–d).

3.1 The abelian diagrams

We start our consideration with the abelian diagrams shown in Figs. 3(a) and (b). In cutting the quark line in all possible ways we obtain a lot of diagrams. However, we find that the final contribution of these diagrams to the soft part of the self energy is suppressed by μ_f^2/m^2 . There can be found different arguments for this suppression. First, in applying the classical Ward identity, the QED diagrams shown in Fig. 4 cancel exactly at $|\vec{k}| \rightarrow 0$, the remaining contribution is of order $O(\vec{k}^2/m^2)$. Concerning this note that the Ward identity for the interaction vertex of a Coulomb gluon with the quark holds even in non-abelian theories [37]. A second argument is that the interaction between a transverse gluon and a non-relativistic quark as shown in Fig. 5(a) is suppressed by μ_f/m , leading to an overall μ_f^2/m^2 suppression. In addition, the box diagrams in Figs. 5(b) and (c) are either suppressed by a factor μ_f^2/m^2 or give an iteration of the leading order potential. To summarize, the diagrams in Figs. 3(a) and (b) give contributions only of the order $g_s^4 \mu_f^2/m^2$.

3.2 The vacuum polarization of the gluon

Following these arguments, it turns out that the only abelian diagrams which can give a non-suppressed contribution to the soft part of the quark self energy are the diagrams containing the vacuum polarization of the gluon as shown in Fig. 3(d–f). The simple calculation of these diagrams within the $\overline{\text{MS}}$ scheme, accounting only for light fermion loops, gluon loop (and ghost

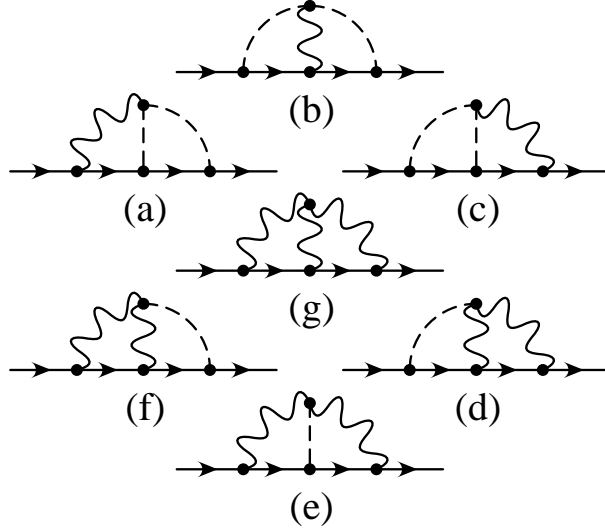


Figure 6: The non-abelian self energy diagram in Coulomb gauge; displayed are Coulomb gluons (wiggles) and transverse gluons (dashed lines)

loop if Feynman gauge is used) results after renormalization in

$$\begin{aligned}
\Sigma_{\text{soft}}^A &= -\frac{1}{2} \int^\mu \frac{d^3k}{(2\pi)^3} \left(-\frac{4\pi\alpha_s(\mu)C_F}{|\vec{k}|^2} \right) \times \\
&\times \left\{ 1 + \frac{\alpha_s(\mu)}{4\pi} \left(\frac{31C_A}{9} - \frac{20T_F N_F}{9} - \left(\frac{11C_A}{3} - \frac{4T_F N_F}{3} \right) \ln \left(\frac{|\vec{k}|^2}{\mu^2} \right) \right) \right\} \\
&= \frac{\alpha_S(\mu)C_F}{\pi} \mu_f \left\{ 1 + \frac{\alpha_s(\mu)}{4\pi} \left(a_1 - \beta_0 \ln \left(\frac{\mu_f^2}{\mu^2} \right) \right) \right\}. \tag{20}
\end{aligned}$$

This result has been anticipated because the expression in the curly brackets of the integrand reproduces the next-to-leading order correction to the QCD Coulomb potential.

3.3 The non-abelian diagram

In this subsection we calculate the non-abelian diagram shown in Fig. 3(c). In Coulomb gauge this diagram gives rise to seven two-loop diagrams which are shown in Fig. 6. Direct calculations show that only the diagram in Fig. 6(b) gives a contribution of order $g_s^4 \mu_f / m$ while the other diagrams are of order $g_s^4 \mu_f^2 / m^2$ or vanish to this order in the coupling after applying the renormalization procedure (see e.g. Ref. [38]). The calculation of the diagram in Fig. 6(b) is simple and we show it in detail. The contribution of this diagram to the self energy is given by

$$\begin{aligned}
-i\Sigma^{6b}(\not{p}) &= \int \frac{d^4k_1}{(2\pi)^4} \frac{d^4k_2}{(2\pi)^4} \frac{i}{\vec{k}_1^2} \frac{i}{\vec{k}_2^2} \frac{i}{(k_1 - k_2)^2} \left(\delta_{ij} - \frac{(k_1 - k_2)_i (k_1 - k_2)_j}{(\vec{k}_1 - \vec{k}_2)^2} \right) g_s f_{abc} (k_1 + k_2)^j g^{00} \times \\
&\times \frac{1 + \gamma^0}{2} (-ig_s \gamma^0 T_a) \frac{i}{\not{p} + \not{k}_2 - m} (-ig_s \gamma^i T_b) \frac{i}{\not{p} + \not{k}_1 - m} (-ig_s \gamma^0 T_c) \frac{1 + \gamma^0}{2}. \tag{21}
\end{aligned}$$

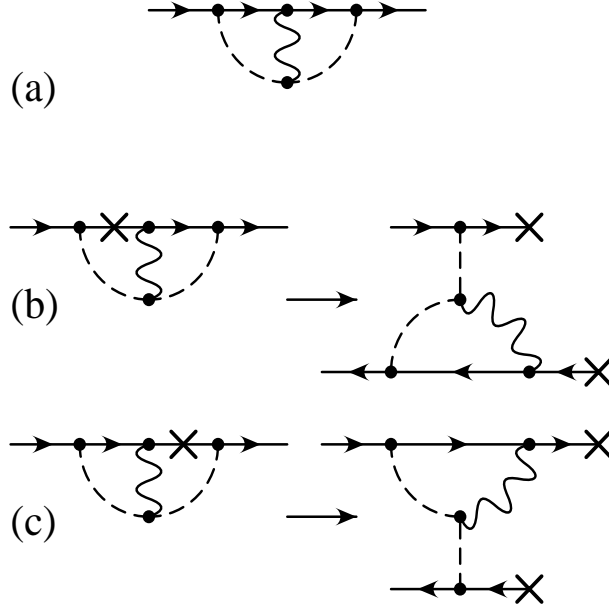


Figure 7: The soft part of the non-abelian diagram under consideration

Here the Lorentz structure of the three-gluon vertex is reduced to $k_1 + k_2$. The Dirac structure of the integrand can be simplified to

$$\frac{1 + \gamma^0}{2} \left\{ -(2m + k_{20}) \gamma^i \vec{k}_1 \vec{\gamma} - \vec{k}_2 \vec{\gamma} \gamma^i (2m + k_{10}) \right\}. \quad (22)$$

The rest of the diagram is symmetric with respect to the interchange of the two line momenta k_1 and k_2 . That provides us with a further simplification of the Dirac structure, the self energy reduces to

$$\Sigma^{6b}(\not{p}) = g_s^4 C_F C_A \int \frac{d^4 k_1}{(2\pi)^4} \frac{d^4 k_2}{(2\pi)^4} \frac{(4m + k_{10} + k_{20}) (\vec{k}_1^2 \vec{k}_2^2 - (\vec{k}_1 \vec{k}_2)^2)}{\vec{k}_1^2 \vec{k}_2^2 (\vec{k}_1 - \vec{k}_2)^2 (k_1 - k_2)^2 ((p + k_1)^2 - m^2) ((p + k_2)^2 - m^2)} \quad (23)$$

where $T_a T_b T_c f_{abc} = i C_F C_A / 2$ has been used. We now employ the replacements

$$\frac{1}{(p + k_1)^2 - m^2} \rightarrow -i\pi \delta((p + k_1)^2 - m^2), \quad \frac{1}{(p + k_2)^2 - m^2} \rightarrow -i\pi \delta((p + k_2)^2 - m^2) \quad (24)$$

i.e. we set cuts at the two intermediate quark lines separately to obtain the two parts $\Sigma_{\text{soft}1}^{6b}$ and $\Sigma_{\text{soft}2}^{6b}$ of the soft contribution $\Sigma_{\text{soft}}^{6b}$ of the self energy, as shown in Fig. 7. Taking the first cut, the delta function removes the integration over k_{10} . At the same time our definition of the soft contribution imposes a restriction $|\vec{k}_1| < \mu_f$ on the space components of the first line momentum. The delta function

$$\delta((p + k_1)^2 - m^2) = \frac{1}{2\sqrt{m^2 + \vec{k}_1^2}} (\delta(k_{10} - k_{1+}) + \delta(k_{10} - k_{1-})) \quad (25)$$

with

$$k_{1\pm} = \pm \sqrt{m^2 + \vec{k}_1^2} - m \quad (26)$$

causes two contributions which are known as scattering and annihilation amplitude (according to k_{1+} and k_{1-} , resp.). The integration over k_{20} is done by using the residue theorem. Actually there are only two denominator factors which can contribute to poles of the integrand, namely $(k_1 - k_2)^2$ and $((p + k_2)^2 - m^2)$. In summing up the four contributions from the integration over k_{20} and k_{10} we end up with a two-fold three-dimensional integral over the space components of the two line momenta where the first integral is restricted by $|\vec{k}_1| < \mu_f$ as mentioned earlier. We now impose the restriction $|\vec{k}_1| < \mu_f$ on the integrand to simplify it and obtain

$$\Sigma_{\text{soft1}}^{6b} = \frac{g_s^4 C_F C_A}{4m} \int^{\mu_f} \frac{d^3 k_1}{(2\pi)^3} \int \frac{d^3 k_2}{(2\pi)^3} \frac{\vec{k}_1^2 \vec{k}_2^2 - (\vec{k}_1 \vec{k}_2)^2}{\vec{k}_1^2 (\vec{k}_2^2)^2 (\vec{k}_1 - \vec{k}_2)^2}. \quad (27)$$

The integral over the space components of k_2 can be easily done by executing the angular integration followed by the radial integration. We obtain

$$\int \frac{d^3 k_2}{(2\pi)^3} \frac{\vec{k}_1^2 \vec{k}_2^2 - (\vec{k}_1 \vec{k}_2)^2}{\vec{k}_1^2 (\vec{k}_2^2)^2 (\vec{k}_1 - \vec{k}_2)^2} = \frac{1}{16|\vec{k}_1|} \quad (28)$$

and therefore, finally

$$\Sigma_{\text{soft1}}^{6b} = \frac{\alpha_s^2 C_F C_A}{16m} \mu_f^2. \quad (29)$$

Symmetry considerations show that $\Sigma_{\text{soft2}}^{6b}$ gives exactly the same contribution. As mentioned before, there are no other non-abelian contributions, therefore we obtain

$$\Sigma_{\text{soft}}^{NA} = \frac{\alpha_s^2 C_F C_A}{8m} \mu_f^2. \quad (30)$$

This result has been anticipated, too, to be minus one half of the non-abelian correction to the QCD Coulomb potential, which is known in the literature (see for example Refs. [39, 53]),

$$\Sigma_{\text{soft}}^{NA} = -\frac{1}{2} \int^{\mu_f} \frac{d^3 k}{(2\pi)^3} \left\{ -\frac{\pi^2 \alpha_s^2 C_F C_A}{m|\vec{k}|} \right\} = \frac{\alpha_s^2 C_F C_A}{8m} \mu_f^2. \quad (31)$$

This calculation concludes the considerations of the two-loop diagrams shown in Fig. 3.

3.4 Our final result

Summarizing all contribution up to NNLO accuracy, we obtain

$$m_{\overline{\text{PS}}}(\mu_f) - m = -\frac{\alpha_s(\mu) C_F}{\pi} \mu_f \left\{ 1 + C_0' \frac{\mu_f}{m} + C_0'' \frac{\mu_f^2}{m^2} + \frac{\alpha_s(\mu)}{4\pi} \left(C_1 + C_1' \frac{\mu_f}{m} \right) + C_2 \left(\frac{\alpha_s(\mu)}{4\pi} \right)^2 \right\} \quad (32)$$

where m is the pole mass, μ is the renormalization scale. This result is considered to be of the order $O(\alpha_s^2)$ because we imply that the ratio μ_f/m is typically of the order of α_s or smaller. The scale μ_f is the factorization scale, and

$$\begin{aligned} C_0 &= 1, & C_0' &= 0, & C_0'' &= -\frac{1}{2}, \\ C_1 &= a_1 - 2\beta_0 \ln\left(\frac{\mu_f}{\mu}\right), & C_1' &= C_A \frac{\pi^2}{2}, \\ C_2 &= a_2 - 2(2a_1\beta_0 + \beta_1) \left(\ln\left(\frac{\mu_f}{\mu}\right) - 1 \right) + 4\beta_0^2 \left(\ln^2\left(\frac{\mu_f}{\mu}\right) - 2 \ln\left(\frac{\mu_f}{\mu}\right) + 2 \right). \end{aligned} \quad (33)$$

The constants a_1 , a_2 , β_0 , and β_1 are given in Appendix A. The coefficients C_1 and C_2 have been derived in Ref. [29] by using known corrections to the QCD potential. In this work we have derived the coefficients C'_0 , C''_0 , and C'_1 . Note that our result can be represented in a condensed form as

$$m_{\overline{\text{PS}}}(\mu_f) - m = -\frac{1}{2} \int^{\mu_f} \frac{d^3k}{(2\pi)^3} \left(V_C(|\vec{k}|) + V_R(|\vec{k}|) + V_{NA}(|\vec{k}|) \right) \quad (34)$$

where the first term V_C is the static Coulomb potential, V_R is the relativistic correction (which is related to Breit-Fermi potential but does not coincide with it), and V_{NA} is the non-abelian correction.

4 Top quark production near threshold with NNLO accuracy

In this section we consider the cross section of the process $e^+e^- \rightarrow t\bar{t}$ in the near threshold region where the velocity v of the top quark is small. It is well-known that the conventional perturbative expansion does not work in the non-relativistic region because of the presence of the Coulomb singularities at small velocities $v \rightarrow 0$. The terms proportional to $(\alpha_s/v)^n$ appear due to the instantaneous Coulomb interaction between the top and the antitop quark. The standard technique for resumming the terms $(\alpha_s/v)^n$ consists in using the Schrödinger equation for the Coulomb potential and to find the Green function [4, 5]. The Green function is then related to the cross section by the optical theorem. In order to determine NLO corrections to the cross section we need to know the short-distance correction to the vector current [42], the NLO correction to the Coulomb potential [43], and the contribution of the non-factorizable corrections [15, 16, 17]. It was proven that the non-factorizable corrections cancel in the inclusive cross section at NLO and beyond [15, 16, 17].

At NNLO the situation is more complicated. One of the obstacles for a straightforward calculation are the UV divergences coming from relativistic corrections to the Coulomb potential. This problem can be solved by a proper factorization of the amplitudes and by employing effective theories. We want to sketch the derivation of the inclusive cross section. The inclusive cross section can be obtained from the correlation function of two vector currents $j_\mu(x) = \bar{t}(x)\gamma_\mu t(x)$,

$$\Pi_{\mu\nu}(p^2) = i \int d^4x e^{ip \cdot x} \langle 0 | T \{ j_\mu(x), j_\nu(0) \} | 0 \rangle. \quad (35)$$

The first step is to expand the Lagrangian and the currents

$$j_i = \bar{t}\gamma_i t = c_1 \psi^\dagger \sigma_i \chi - \frac{c_2}{6m^2} \psi^\dagger \sigma_i (i\vec{D})^2 \chi, \quad (36)$$

consistently in $1/m$. The useful language for treating the one and two non-relativistic quark(s) is provided by the NRQCD [44, 45] and the PNRQCD [46], respectively. After the expansion, the relative cross section reads

$$R = \sigma(e^+e^- \rightarrow t\bar{t})/\sigma_{pt} = e_Q^2 N_c \frac{24\pi}{s} C(r_0) \text{Im} \left[\left(1 - \frac{\vec{p}^2}{3m^2} \right) G(r_0, r_0 | E + i\Gamma) \right] \Big|_{r_0 \rightarrow 0} \quad (37)$$

where $\sigma_{pt} = 4\pi\alpha^2/3s$, e_Q is the electric charge of the top quark, N_c is the number of colors, $\sqrt{s} = 2m + E$ is the total center-of-mass energy of the quark-antiquark system, m is the top

quark pole mass and Γ is the top quark width. The unknown coefficient $C(r_0)$ can be fixed by using a direct QCD calculation of the vector vertex at NNLO in the so-called intermediate region [47, 48] and by using the direct matching procedure suggested in Ref. [49]. The result of such a matching procedure for the coefficient $C(r_0)$ is given in the Appendix [19, 20, 21, 22].

The function $G(\vec{r}, \vec{r}'|E + i\Gamma)$ is the non-relativistic Green function. It satisfies the Schrödinger equation

$$(H - E - i\Gamma)G(\vec{r}, \vec{r}'|E + i\Gamma) = \delta(\vec{r} - \vec{r}'). \quad (38)$$

The non-relativistic Hamiltonian of the heavy quark-antiquark system reads

$$H = H_0 + W(r), \quad H_0 = \frac{\vec{p}^2}{m} + V_C(r), \quad (39)$$

where $V_C(r)$ is the static QCD potential of the heavy quark-antiquark system at NNLO order,

$$V_C(r) = -\frac{\alpha_s(\mu)C_F}{r} \left\{ 1 + \frac{\alpha_s(\mu)C_F}{4\pi} (2\beta_0 \ln(\mu'r) + a_1) + \left(\frac{\alpha_s(\mu)}{4\pi} \right)^2 \left(\beta_0^2 \left(4\ln^2(\mu'r) + \frac{\pi^2}{3} \right) + 2(\beta_1 + 2\beta_0 a_1) \ln(\mu'r) + a_2 \right) \right\}, \quad (40)$$

$\mu' = \mu e^{\gamma_E}$, μ is the renormalization scale, and γ_E is Euler's constant. The color factors are given by $C_F = 4/3$, $C_A = 3$ and $T_F = 1/2$. The number of light quark flavors is $N_F = 5$. The coefficients a_1 and a_2 were calculated in [50] and [51, 52], respectively, and are listed in the Appendix.

The function $W(r)$ in Eq. (39) is the QCD generalization of the QED Breit-Fermi Hamiltonian [36, 39, 53]. We consider here the quark-antiquark production in the S -wave mode. The Breit-Fermi Hamiltonian for the final state with $\vec{L} = 0$, $\vec{S}^2 = 2$ reads

$$W(r) = -\frac{\vec{p}^4}{4m^3} + \frac{11\pi C_F \alpha_s(\mu)}{3m^2} \delta(\vec{r}) - \frac{C_F \alpha_s(\mu)}{2m^2} \left\{ \frac{1}{r}, \vec{p}^2 \right\} - \frac{C_A C_F \alpha_s^2(\mu)}{2mr^2}. \quad (41)$$

It has been demonstrated in Refs. [19, 20, 21] that the Schrödinger equation can be reduced to the equation

$$(H_1 - E_1)G_1(r, r'|E_1) = \delta^3(r - r') \quad (42)$$

with the energy $E_1 = \bar{E} + \bar{E}^2/4m$, $\bar{E} = E + i\Gamma$, and with the Hamiltonian

$$H_1 = \frac{\vec{p}^2}{m} + V_C(r) + \frac{3\bar{E}}{2m} V_0(r) - \left(\frac{2}{3} + \frac{C_A}{C_F} \right) \frac{V_0^2(r)}{2m}, \quad V_0(r) = -\frac{\alpha_s(\mu)C_F}{r}. \quad (43)$$

The final expression for the NNLO cross section is given by

$$R^{\text{NNLO}}(E) = \frac{8\pi}{m^2} \left\{ 1 - 4C_F \frac{\alpha_s(m)}{\pi} + C_2(r_0)C_F \left(\frac{\alpha_s(m)}{\pi} \right)^2 \right\} \text{Im} \left[\left(1 - \frac{5\bar{E}}{6m} \right) G_1(r_0, r_0|E_1) \right] \quad (44)$$

with $G_1(r_0, r_0|E_1)$ being the solution of Eq. (42) at $r = r' = r_0$ while $C_2(r_0)$ is taken from Eqs. (A3–A5). For the numerical solution we use the program derived in Ref. [21] by one of the authors.

$\overline{m}(\overline{m})$	$m_{\overline{\text{PS}}}^{\text{LO}}$	$m_{\overline{\text{PS}}}^{\text{NLO}}$	$m_{\overline{\text{PS}}}^{\text{NNLO}}$ $m_{\overline{\text{PS}}}^{\text{NNLO}}$	$m_{\overline{\text{PS}}}^{\beta_0}$ $m_{\overline{\text{PS}}}^{\beta_0}$	$m_{\text{pole}}^{\text{LO}}$	$m_{\text{pole}}^{\text{NLO}}$	$m_{\text{pole}}^{\text{NNLO}}$	$m_{\text{pole}}^{\beta_0}$
160.0	166.51	167.69	167.97 167.95	168.05 168.03	167.44	169.05	169.56	169.80
165.0	171.72	172.93	173.22 173.20	173.30 173.28	172.64	174.28	174.80	175.05
170.0	176.92	178.17	178.47 178.45	178.55 178.53	177.84	179.52	180.05	180.30

Table 1: Top quark mass relations for the $\overline{\text{MS}}$, PS, $\overline{\text{PS}}$, and the pole mass at LO, NLO, NNLO, and “large β_0 ” accuracy in GeV. We fix the $\overline{\text{MS}}$ mass to be $\overline{m}(\overline{m}) = 160$ GeV, 165 GeV, and 170 GeV and find the pole mass at LO, NLO, and NNLO from the three-loop relation in Eq. (45). The PS and $\overline{\text{PS}}$ masses are derived from the pole mass by using Eq. (32) (without or with the $1/m$ contributions, respectively). We use the QCD coupling constant $\alpha_s(m_Z) = 0.119$ [56], $\mu = \overline{m}(\overline{m})$, and $\mu_f = 20$ GeV for the factorization scale in the PS and $\overline{\text{PS}}$ masses.

4.1 Relations between the masses

Our main result is Eq. (32), it enables us to relate the pole mass to the $\overline{\text{PS}}$ mass or the PS mass (the latter by leaving out the terms of higher order in $1/m$). Note that we did not include electroweak corrections neither in this mass relation nor in the cross section. To relate the pole mass to the $\overline{\text{MS}}$ mass we use the three-loop relation which has been derived in Ref. [54, 55],

$$\begin{aligned} \frac{m_{\text{pole}}}{\overline{m}(\overline{m})} &= 1 + \frac{4}{3} \left(\frac{\alpha_s}{\pi} \right) + \left(\frac{\alpha_s}{\pi} \right)^2 (-1.0414N_F + 13.4434) \\ &\quad + \left(\frac{\alpha_s}{\pi} \right)^3 (0.6527N_F^2 - 26.655N_F + 190.595) \end{aligned} \quad (45)$$

where $\alpha_s = \alpha_s(\overline{m})$ is taken at the $\overline{\text{MS}}$ mass. More precisely, we fix the $\overline{\text{MS}}$ mass to take the values $\overline{m}(\overline{m}) = 160$ GeV, 165 GeV, and 170 GeV and use Eq. (45) to determine the pole mass at LO, NLO, and NNLO. This pole mass is then used as input parameter m in Eq. (32) to determine the PS and $\overline{\text{PS}}$ masses at LO, NLO, and NNLO. The obtained values for the PS and the $\overline{\text{PS}}$ mass differ only in NNLO. The results of these calculations are collected in Table 1, together with the estimates for “large β_0 ” accuracy [40, 41]. Note that the same values for the $\overline{\text{MS}}$ mass have been used for Tables 2 and 3 in Ref. [26]. The obtained mass values can now be used for an analysis of the Schrödinger equation.

Taking the $\overline{\text{PS}}$ mass instead of the PS mass, we observe an improvement of the convergence. The differences for the mass values in going from LO to NLO to NNLO to the “large β_0 ” estimate for e.g. $\overline{m}(\overline{m}) = 165$ GeV read 7.64 GeV, 1.64 GeV, 0.52 GeV, and 0.25 GeV for the pole mass, 6.72 GeV, 1.21 GeV, 0.29 GeV, and 0.08 GeV for the PS mass and finally 6.72 GeV, 1.21 GeV, 0.27 GeV, and 0.08 GeV for the $\overline{\text{PS}}$ mass.

In Fig. 8 we show the difference between the $\overline{\text{PS}}$ and the PS mass (in GeV) as a function of the factorization scale μ_f (solid line) at $\mu = 15$ GeV. It is interesting to observe that the

non-abelian part of the difference between the $\overline{\text{PS}}$ and the PS mass (dotted line in Fig. 8) can be as large as 200 MeV. But the recoil correction cancel in part the non-abelian one and therefore the final difference is not more than 50 MeV. The dependence of $m_{\overline{\text{PS}}} - m_{\text{PS}}$ on the renormalization scale at $\mu_f = 30$ GeV is given in Fig. 8 by the dashed curve.

4.2 The concept with the pole mass

The top quark cross section at LO, NLO, and NNLO is shown in Fig. 9 as a function of the center-of-mass energy. For the top quark pole mass we use $m_t = 175.05$ GeV, for the top quark width $\Gamma_t = 1.43$ GeV, and for the QCD coupling constant $\alpha_s(m_Z) = 0.119$ [56]. Different values $\mu = 15$ GeV, 30 GeV, and 60 GeV for the renormalization scale are selected because they roughly correspond to the typical spatial momenta for the top quark. For solving the Schrödinger equation we use the program written by one of the authors [21]. Note that we do not take into account an initial photon radiation which would change the shape of the cross section. This can be easily included in the Monte Carlo simulation.

The NNLO curve modifies the line shape by the amount of 20 – 30% which is as large as the NLO correction. It also shifts the position of the $1S$ peak by approximately 600 MeV. These large shifts of the peak position were expected. As we discussed above (and is well-known in the literature [27, 28]), the pole mass definition suffers from the renormalon ambiguity. The top quark pole mass cannot be defined better than $O(\Lambda_{\text{QCD}})$. Large NNLO corrections and a large shift of the $1S$ resonance can spoil the top quark mass measurement at the NLC.

4.3 The concept with the PS mass

In this subsection we discuss the calculation concept using the PS mass. We redefine the pole mass through the PS mass using the relation given in Eq. (32) without the $1/m$ contributions and then use the PS mass as an input parameter for our numerical analysis at LO, NLO, and NNLO. In Fig. 10 we show the top quark cross section expressed in terms of $m_{\text{PS}}(\mu_f)$ at LO, NLO, and NNLO (like in Fig. 9) as a function of the center-of-mass energy. We take $m_{\text{PS}}(\mu_f = 20 \text{ GeV}) = 173.30$ GeV which corresponds to the pole mass $m = 175.05$ GeV according to Table 1. In looking at Fig. 10 we observe an improvement in the stability of the position of the first peak in comparison to the previous analysis as we go from LO to NLO to NNLO. Actually, for the three values $\mu = 15$ GeV, 30 GeV, and 60 GeV we obtain the maxima of the $1S$ peak for NNLO at $s_{\text{max}} = 347.32$ GeV, 347.41 GeV, and 347.48 GeV while the maximal values are given by $R_{\text{max}} = 1.379$, 1.184, and 1.088, respectively. This demonstrated that a large variation in the renormalization scale μ gives rise only to a shift of about 160 MeV for the $1S$ peak position at NNLO while the variation for R_{max} is still large.

4.4 The concept with the $\overline{\text{PS}}$ mass

In this subsection we discuss the calculation concept where we use the $\overline{\text{PS}}$ mass. We redefine the pole mass through the $\overline{\text{PS}}$ mass by using the relation given in Eq. (32) and then use the $\overline{\text{PS}}$ mass as an input parameter for the numerical analysis at LO, NLO, and NNLO. In Fig. 11 we show the top quark cross section expressed in terms of $m_{\overline{\text{PS}}}(\mu_f)$ at LO, NLO, and NNLO (like in Fig. 9) as a function of the center-of-mass energy. We take $m_{\overline{\text{PS}}}(\mu_f = 20 \text{ GeV}) = 173.28$ GeV. Again we observe a very good stability of the position of the first peak as we go from LO to NLO to NNLO, similar to the one observed for the PS mass case. Studying the size of the

NNLO corrections to the peak positions we conclude that the current theoretical uncertainty of the determination of the PS mass from the $1S$ peak position is about $100 - 200$ MeV.

5 Conclusion and discussions

We introduced the so-called $\overline{\text{PS}}$ mass which is an infrared-insensitive quark mass, naturally defined by subtracting the soft part of the quark self energy from the pole mass. We demonstrated a deep relation of this definition with the static quark-antiquark potential. At leading order in $1/m$ the $\overline{\text{PS}}$ mass coincides with the PS mass, defined in a completely different manner. In contrast to the pole mass, the $\overline{\text{PS}}$ mass is not sensitive to the non-perturbative QCD effects. Going beyond the static limit, the small normalization point introduces recoil corrections to the relation of the pole mass with the $\overline{\text{PS}}$ mass which have been calculated in this paper. In addition we demonstrated that, if we use the PS or the $\overline{\text{PS}}$ mass in the calculations, the perturbative predictions for the cross section become much more stable at higher orders of QCD (shifts are below 0.1 GeV). This understanding removes one of the obstacles for an accurate top mass measurement and one can expect that the top quark mass will be extracted from a threshold scan at NLC with an accuracy of about $100 - 200$ MeV.

Acknowledgements: We are grateful to Ratindranath Akhoury, Ed Yao and Martin Beneke for valuable discussions. O.Y. acknowledges support from the US Department of Energy (DOE). S.G. acknowledges a grant given by the DFG, FRG, he also would like to thank the members of the theory group at the Newman Lab for their hospitality during his stay.

Appendix

The coefficients a_1 and a_2 were calculated in Refs. [50] and [51, 52], respectively, and are given by

$$\begin{aligned} a_1 &= \frac{31}{9}C_A - \frac{20}{9}T_F N_F, \\ a_2 &= \left(\frac{4343}{162} + 4\pi^2 - \frac{\pi^4}{4} + \frac{22}{3}\zeta_3 \right) C_A^2 - \left(\frac{1798}{81} + \frac{56}{3}\zeta_3 \right) C_A T_F N_F \\ &\quad + \left(\frac{20}{9}T_F N_F \right)^2 - \left(\frac{55}{3} - 16\zeta_3 \right) C_F T_F N_F. \end{aligned} \quad (\text{A1})$$

The first two coefficients in the expansion of the QCD β -function are

$$\beta_0 = \frac{11}{3}C_A - \frac{4}{3}T_F N_F, \quad \beta_1 = \frac{34}{3}C_A^2 - \frac{20}{3}C_A T_F N_F - 4C_F T_F N_F. \quad (\text{A2})$$

The short distance coefficient reads

$$\begin{aligned} C(r) &= 1 - 4C_F \frac{\alpha_s(\mu_h)}{\pi} + C_2(r) C_F \left(\frac{\alpha_s(\mu_h)}{\pi} \right)^2, \\ C_2(r) &= A_1 \log(r/a) + A_2 \log(m/\mu_h) + A_3 \end{aligned} \quad (\text{A3})$$

where the hard renormalization scale is taken to be the pole mass, $\mu_h = m$, $a = e^{2-\gamma_E}/2m$, and

$$\begin{aligned} A_1 &= \pi^2 \left(C_A + \frac{2C_F}{3} \right), \quad A_2 = 2\beta_0, \\ A_3 &= C_2^A C_F + C_2^{NA} C_A + C_2^L T_F N_F + C_2^H T_F \end{aligned} \quad (\text{A4})$$

where $N_F = 5$ is the number of the light flavors, and

$$\begin{aligned}
C_2^A &= \frac{39}{4} - \zeta_3 + \pi^2 \left(\frac{4}{3} \ln 2 - \frac{35}{18} \right), \\
C_2^{NA} &= -\frac{151}{36} - \frac{13}{2} \zeta_3 + \pi^2 \left(\frac{179}{72} - \frac{8}{3} \ln 2 \right), \\
C_2^L &= \frac{11}{9}, \quad C_2^H = \frac{44}{9} - \frac{4}{9} \pi^2.
\end{aligned} \tag{A5}$$

References

- [1] F. Abe *et al.*, [CDF Collaboration] Phys. Rev. Lett. **74** (1995) 2626 [hep-ex/9503002]
S. Abachi *et al.*, [D0 Collaboration] Phys. Rev. Lett. **74** (1995) 2632 [hep-ex/9503003]
- [2] G. Brooijmans [CDF and D0 Collaborations],
“Top quark mass measurements at the Tevatron” [hep-ex/0005030]
- [3] M.E. Peskin, “Physics goals of the linear collider” [hep-ph/9910521]
- [4] V.S. Fadin and V.A. Khoze, JETP Lett. **46** (1987) 525
- [5] V.S. Fadin and V.A. Khoze, Sov. J. Nucl. Phys. **48** (1988) 309
- [6] E.C. Poggio, H.R. Quinn and S. Weinberg, Phys. Rev. **D13** (1976) 1958
- [7] M.J. Strassler and M.E. Peskin, Phys. Rev. **D43** (1991) 1500
- [8] V.S. Fadin and O. Yakovlev, Sov. J. Nucl. Phys. **53** (1991) 688
- [9] W. Kwong, Phys. Rev. **D43** (1991) 1488
- [10] M. Jezabek, J.H. Kühn and T. Teubner, Z. Phys. **C56** (1992) 653
- [11] Y. Sumino, K. Fujii, K. Hagiwara, H. Murayama and C.K. Ng,
Phys. Rev. **D47** (1993) 56
- [12] R.J. Guth and J.H. Kühn, Nucl. Phys. **B368** (1992) 38
- [13] W. Beenakker and W. Hollik, Phys. Lett. **269 B** (1991) 425
- [14] V.S. Fadin and O. Yakovlev, Sov. J. Nucl. Phys. **53** (1991) 1053;
Sov. J. Nucl. Phys. **50** (1989) 1037
- [15] K. Melnikov and O. Yakovlev, Phys. Lett. **324 B** (1994) 217 [hep-ph/9302311]
- [16] V.S. Fadin, V.A. Khoze and A.D. Martin, Phys. Rev. **D49** (1994) 2247
- [17] V.S. Fadin, V.A. Khoze and A.D. Martin, Phys. Lett. **320 B** (1994) 141 [hep-ph/9309234]
- [18] Y. Sumino, PhD thesis, Tokyo University, Report No. UT-655, 1993
- [19] A.H. Hoang and T. Teubner, Phys. Rev. **D58** (1998) 114023 [hep-ph/9801397]

- [20] K. Melnikov and A. Yelkhovsky, Nucl. Phys. **B528** (1998) 59 [hep-ph/9802379]
- [21] O. Yakovlev, Phys. Lett. **457 B** (1999) 170 [hep-ph/9808463]
- [22] M. Beneke, A. Signer and V.A. Smirnov, Phys. Lett. **454 B** (1999) 137 [hep-ph/9903260]
- [23] A.H. Hoang and T. Teubner, Phys. Rev. **D60** (1999) 114027 [hep-ph/9904468]
- [24] T. Nagano, A. Ota and Y. Sumino, Phys. Rev. **D60** (1999) 114014 [hep-ph/9903498]
- [25] A.A. Penin and A.A. Pivovarov, “Analytical results for $e^+e^- \rightarrow t\bar{t}$ and $\gamma\gamma \rightarrow t\bar{t}$ observables near the threshold up to the next-to-next-to-leading order of NRQCD” [hep-ph/9904278]
- [26] A.H. Hoang *et al.*, Eur. Phys. J. direct **C3** (2000) 1 [hep-ph/0001286]
- [27] M. Beneke and V.M. Braun, Nucl. Phys. **B426** (1994) 301 [hep-ph/9402364]
- [28] I.I. Bigi, M.A. Shifman, N.G. Uraltsev and A.I. Vainshtein, Phys. Rev. **D50** (1994) 2234 [hep-ph/9402360]
- [29] M. Beneke, Phys. Lett. **434 B** (1998) 115 [hep-ph/9804241]
- [30] N. Uraltsev, “Heavy-quark expansion in beauty and its decays”, talk given at the International School of Physics, “Enrico Fermi: Heavy Flavor Physics – A Probe of Nature’s Grand Design”, Varenna, Italy, July 8–18, 1997, In “Varenna 1997, Heavy flavor physics”, p. 329 [hep-ph/9804275]
- [31] A. Czarnecki, K. Melnikov and N. Uraltsev, Phys. Rev. Lett. **80** (1998) 3189 [hep-ph/9708372]
- [32] A.H. Hoang and T. Teubner, Phys. Rev. **D60** (1999) 114027 [hep-ph/9904468]
- [33] O. Yakovlev, talk given at the Mini-Workshop on “Physics at the $t\bar{t}$ threshold”, Karlsruhe, Germany, Dec. 20, 1998; talk given at the Workshop on “Physics at NLC”, Berkeley, California, March 2000.
- [34] K. Melnikov, talk given at the Mini-Workshop on “Physics at the $t\bar{t}$ threshold”, Karlsruhe, Germany, Dec. 20, 1998.
- [35] A.H. Hoang, M.C. Smith, T. Stelzer and S. Willenbrock, Phys. Rev. **D59** (1999) 114014 [hep-ph/9804227]
- [36] V.B. Berestetskii, E.M. Lifshitz, L.P. Pitaevskii, “Relativistic Quantum Theory”, Pergamon Press (1971), Volume 4, part 1, page 280
- [37] F. Feinberg, Phys. Rev. **D17** (1978) 2659
- [38] W. Kummer and W. Mödritsch, Z. Phys. **C66** (1995) 225 [hep-ph/9408216]
- [39] S.N. Gupta and F. Radford, Phys. Rev. **D24** (1981) 2309; **D25** (1982) 3430; S.N. Gupta, F. Radford and W.W. Repko, Phys. Rev. **D26** (1982) 3305
- [40] U. Aglietti and Z. Ligeti, Phys. Lett. **364 B** (1995) 75 [hep-ph/9503209]

- [41] M. Beneke and V.M. Braun, Phys. Lett. **348 B** (1995) 513 [hep-ph/9411229]
- [42] R. Karplus and A. Klein, Phys. Rev. **87** (1952) 848
- [43] A. Billoire, Phys. Lett. **92 B** (1980) 343
- [44] W.E. Caswell and G.P. Lepage, Phys. Lett. **167 B** (1986) 437
- [45] G.T. Bodwin, E. Braaten and G.P. Lepage, Phys. Rev. **D51** (1995) 1125 [hep-ph/9407339]
- [46] A. Pineda and J. Soto, Phys. Rev. **D59** (1999) 016005 [hep-ph/9805424]
- [47] A. Czarnecki and K. Melnikov, Phys. Rev. Lett. **80** (1998) 2531 [hep-ph/9712222]
- [48] M. Beneke and V.A. Smirnov, Nucl. Phys. **B522** (1998) 321 [hep-ph/9711391];
M. Beneke, A. Signer and V.A. Smirnov, Phys. Rev. Lett. **80** (1998) 2535 [hep-ph/9712302]
- [49] A.H. Hoang, Phys. Rev. **D56** (1997) 5851; Phys. Rev. **D57** (1998) 1615
- [50] W. Fischler, Nucl. Phys. **B129** (1977) 157
- [51] M. Peter, Nucl. Phys. **B501** (1997) 471 [hep-ph/9702245]
- [52] Y. Schröder, Phys. Lett. **447 B** (1999) 321 [hep-ph/9812205]
- [53] A. Duncan, Phys. Rev. **D13** (1973) 2866
- [54] K. Melnikov and T. van Ritbergen, Phys. Lett. **482 B** (2000) 99 [hep-ph/9912391]
- [55] K.G. Chetyrkin and M. Steinhauser, Phys. Rev. Lett. **83** (1999) 4001 [hep-ph/9907509];
Nucl. Phys. **B573** (2000) 617 [hep-ph/9911434]
- [56] Particle Data Group (C. Caso *et al.*), Eur. Phys. J. **C3** (1998) 1

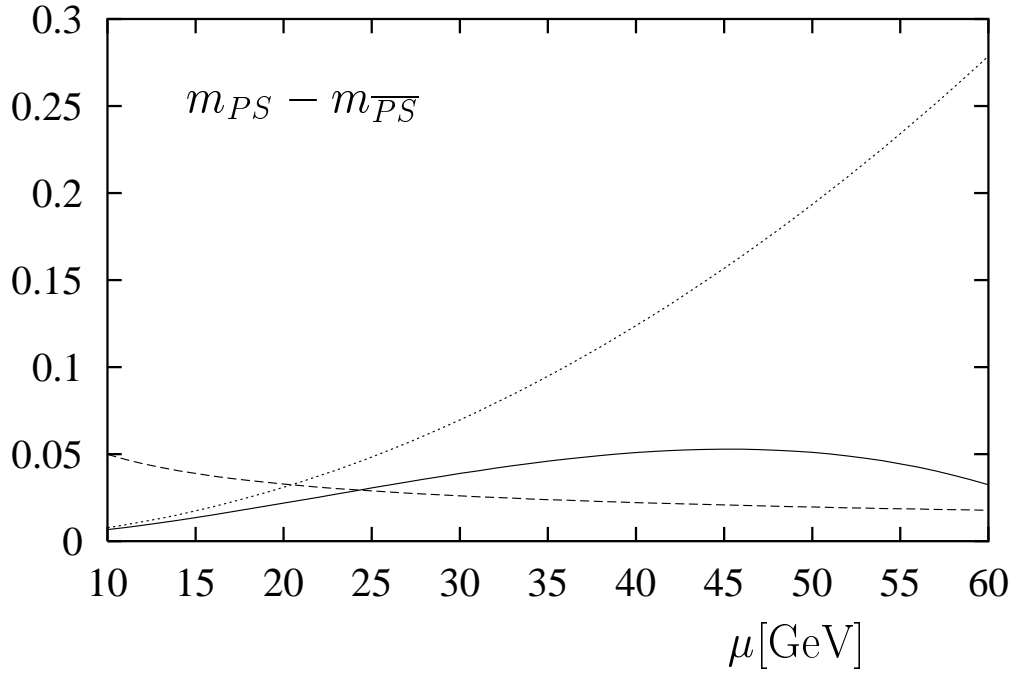


Figure 8: The difference between the PS and the \overline{PS} mass (in GeV) as a function of the factorization scale μ_f (solid line) at $\mu = 15$ GeV. The dotted line shows only the non-abelian part of the difference. The dependence of $m_{\overline{PS}} - m_{PS}$ as a function of the normalization scale μ at $\mu_f = 30$ GeV is shown as dashed line.

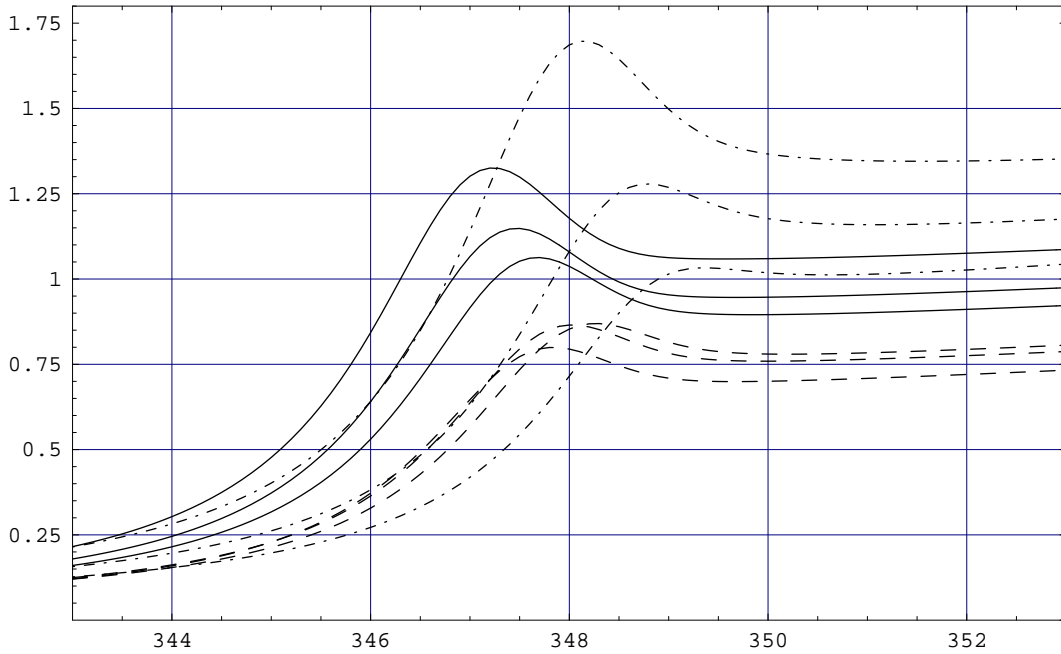


Figure 9: The concept using the pole mass: shown is the relative cross section $R(e^+e^- \rightarrow t\bar{t})$ as a function of the center-of-mass energy in GeV for the LO (dashed-dotted lines), NLO (dashed lines), and NNLO (solid lines) approximation. We take the value $m_t = 175.05$ GeV for the pole mass of the top quark, $\Gamma_t = 1.43$ GeV for the top quark width, $\alpha_s(m_Z) = 0.119$ and different values $\mu = 15$ GeV, 30 GeV, and 60 GeV for the renormalization scale.

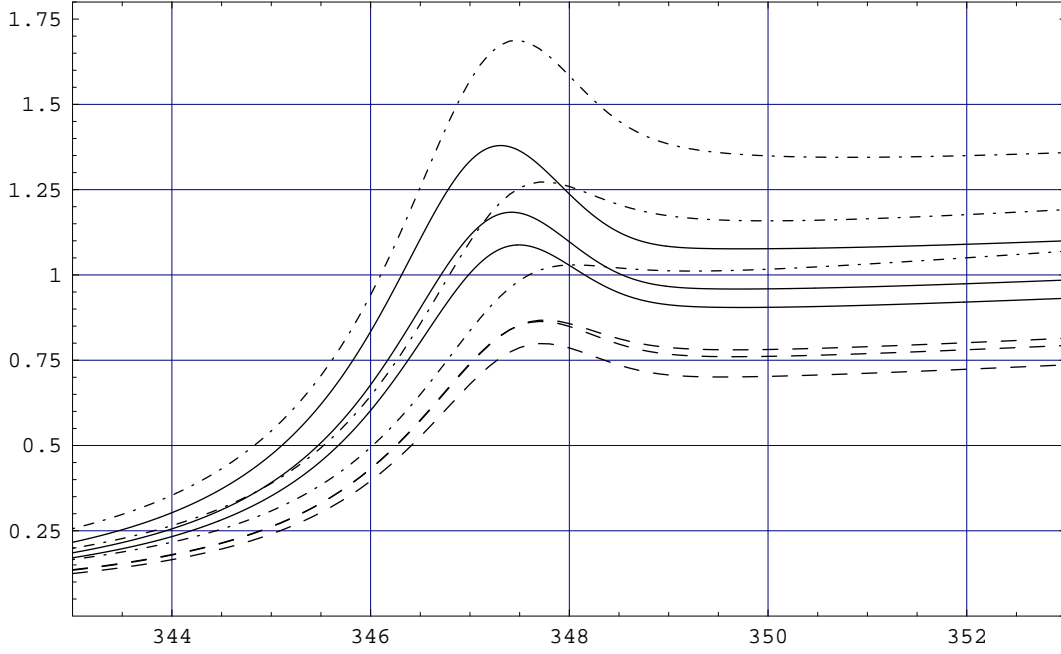


Figure 10: The concept using the PS mass: shown is the relative cross section $R(e^+e^- \rightarrow t\bar{t})$ as a function of the center-of-mass energy in GeV for the LO (dashed-dotted lines), NLO (dashed lines), and NNLO (solid lines) approximation. We take the value $m_{\text{PS}} = 173.30$ GeV for the PS mass of the top quark, $\Gamma_t = 1.43$ GeV for the top quark width, $\alpha_s(m_Z) = 0.119$ and different values $\mu = 15$ GeV, 30 GeV, and 60 GeV for the renormalization scale.

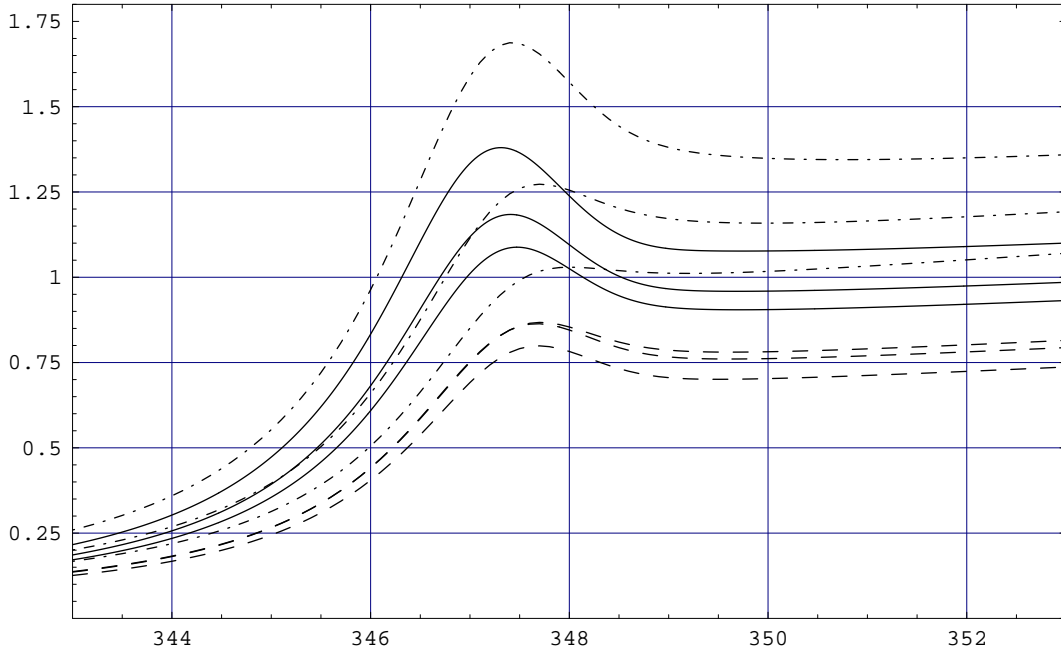


Figure 11: The concept using the $\overline{\text{PS}}$ mass: shown is the relative cross section $R(e^+e^- \rightarrow t\bar{t})$ as a function of the center-of-mass energy in GeV for the LO (dashed-dotted lines), NLO (dashed lines), and NNLO (solid lines) approximation. We take the value $m_{\overline{\text{PS}}} = 173.28$ GeV for the $\overline{\text{PS}}$ mass of the top quark, $\Gamma_t = 1.43$ GeV for the top quark width, $\alpha_s(m_Z) = 0.119$ and different values $\mu = 15$ GeV, 30 GeV, and 60 GeV for the renormalization scale.